Analyst

Dynamic Article Links

Cite this: *Analyst*, 2012, **137**, 3635

www.rsc.org/analyst

PAPER

Monitoring of chicken meat freshness by means of a colorimetric sensor array

Yolanda Salinas,[ad] José V. Ros-Lis,*[a] José-L. Vivancos,[acd] Ramón Martínez-Máñez,*[abd] M. Dolores Marcos,[abd] Susana Aucejo,[e] Nuria Herranz[e] and Inmaculada Lorente[e]

Received 14th February 2012, Accepted 5th June 2012
DOI: 10.1039/c2an35211g

A new optoelectronic nose to monitor chicken meat ageing has been developed. It is based on 16 pigments prepared by the incorporation of different dyes (pH indicators, Lewis acids, hydrogen-bonding derivatives, selective probes and natural dyes) into inorganic materials (UVM-7, silica and alumina). The colour changes of the sensor array were characteristic of chicken ageing in a modified packaging atmosphere (30% CO_2–70% N_2). The chromogenic array data were processed with qualitative (PCA) and quantitative (PLS) tools. The PCA statistical analysis showed a high degree of dispersion, with nine dimensions required to explain 95% of variance. Despite this high dimensionality, a tridimensional representation of the three principal components was able to differentiate ageing with 2-day intervals. Moreover, the PLS statistical analysis allows the creation of a model to correlate the chromogenic data with chicken meat ageing. The model offers a PLS prediction model for ageing with values of 0.9937, 0.0389 and 0.994 for the slope, the intercept and the regression coefficient, respectively, and is in agreement with the perfect fit between the predicted and measured values observed. The results suggest the feasibility of this system to help develop optoelectronic noses that monitor food freshness.

1. Introduction

It is well-established that a country's meat consumption increases in accordance with its degree of development. Among the various kinds of meat, poultry is the second most consumed in the world after pork (more than 75 millions of tons per year), with an annual consumption at round 30 kg per person.[1] There are several reasons to explain the success of poultry meat: its low price, white meat is considered healthier than red meat, chickens grow easily, its plain taste makes it acceptable in different countries and cultures, and its use in prepared meals as an inexpensive source of proteins. However, chicken meat also has its disadvantages: its comparatively short shelf life, plus the presence of bacteria derived from the original microflora and meat processing conditions. Meat ageing, in addition to producing high levels of biogenic amines, is often accompanied by bacterial toxins and metabolites that may render food unsafe for consumption regardless of any toxic effects of the biogenic amines present. Several methods have been developed to prolong the freshness period, including dipping chicken in reagents,[2] or the use of radiation or vacuum. Probably one of the most common systems, which is more readily accepted by consumers for its use in self-service packages, is the combination of refrigeration and modified atmosphere packaging (MAP).[3] Unfortunately in most cases, the latter does not provide individualised knowledge of freshness by mere visual inspection to alert eventual alterations of the cooling chain or contamination during the packaging process. In fact, consumers' concern about meat freshness is continually increasing. Hence, simple-to-use reliable methods for meat freshness assessment and/or microbiological quality would benefit both consumers and the meat industry.

Spoilage is observed when food becomes undesirable for human consumption caused by organoleptic changes, including variations in appearance (slime, discolouration) or development of off-odours and/or off-flavours. Fresh meat is a complex issue where many biological processes occur depending on the storage time, packaging conditions, microbial loading, humidity, *etc.* In the particular case of chicken, spoilage at refrigeration temperatures is attributed mainly to microbial by-products and not to autolytic products originating from the tissue.[4] Current analysis methods to determine chicken ageing include the use of microbiological techniques, sensorial panels, microscopy, detection of metabolite concentrations (*i.e.*, ATP, glucose and derived compounds or biogenic amines),[5] ion mobility spectrometry (IMS), NIR and fluorescence spectroscopy,[6] and electronic tongues and noses.[7] Despite the accuracy of some of these

[a]*Centro de Reconocimiento Molecular y Desarrollo Tecnológico, Unidad Mixta UniversitatPolitècnica de València-Universitat de València, Spain. E-mail: rmaez@qim.upv.es; joroli@upv.es; Fax: +34 963879349; Tel: +34 963879347*
[b]*Departamento de Química, UniversitatPolitècnica de València, Camino de Vera s/n, 46021 València, Spain*
[c]*Departamento de Proyectos de Ingeniería, UniversitatPolitècnica de València, Camino de Vera s/n, 46021 València, Spain*
[d]*CIBER de Bioingeniería, Biomateriales y Nanomedicina (CIBER-BBN)*
[e]*ITENE Packaging, Transport & Logist Res Ctr, C Albert Einstein 1, València 46980, Spain*

methods, they are usually destructive, time-consuming, employ expensive instrumentation, require qualified personnel or cannot be used for *in situ* determinations. These procedures are generally suitable for food safety agencies, but not for use in supermarkets, at consumers' homes or in every piece of meat. Although a use-by date is incorporated into the package, this is a generic approach that does not inform about the particular state of every package, and proves invalid to report improper meat treatment during distribution or differences in end users handling. If we bear this particular aspect in mind, the development of disposable systems capable of being incorporated into the package to offer individual easy-to-interpret information on freshness by end users may be of much importance.

Among the techniques that develop easy handling disposable systems, the use of chromogenic chemosensors[8] is, perhaps, one of the most promising since they are usually cheap, versatile, can be printed on the package, colour changes can be easily measured using cameras or other image capturing systems, and in certain circumstances, they may allow the naked eye detection of colour changes through transparent films. Few technologies are as advanced or as inexpensive as visual imaging. Although some chromogenic indicators have been described[9,10] they are generally based on a single compound and have some limitations such as lack of specificity (offering false positives or false negatives). Additionally, the presence of certain target metabolites is not necessarily an indication of poor quality. More exact correlations seem to be necessary among target metabolites, product type and organoleptic quality and safety. The possibility of false negatives is likely to dissuade producers from adopting indicators unless specific indications of actual spoilage can be guaranteed. Another innovative approach includes time temperature indicators (TTI),[9] which inform about any temperature above a limit through colour changes. Although some correlations can be established between temperature and freshness, they do not really provide information about the biochemical processes occurring in food. Thus, although some attempts have been made in single analyte indicators, the most promising, potent and versatile approach to be applied in complex matrixes is the use of optoelectronic noses, built by an array of dyes able to offer information through suitable colour changes.[11,12] Indeed in the last few years, the use of arrays of non-specific sensors has proved a suitable approach to analyse complex systems, and a number of examples of electronic noses and tongues can be found in the literature, unlike examples of chromogenic arrays that are scarcer.[13] Based on the above issues, and following our general interest in developing colorimetric probes,[14] we report herein a prospective study of using an array of chromogenic indicators with different chemical recognition properties, which we have applied to follow the evolution of chicken ageing.

2. Experimental

2.1 Chemicals

Phenol red, bromocresol purple, dimethyl yellow, carminic acid, curcumin from curcuma, *m*-cresol purple, litmus, malachite green, phenolphthalein, aluminium oxide and silica gel were purchased from Sigma-Aldrich and analytical-grade solvents were acquired from Scharlab. All the reagents were used as received with no further purification. 2,6-Diphenyl-4-(2-(4-*N*,*N*-dimethylaminophenyl)vinyl)-pyrylium tetrafluoroborate,[15] 4-(4-*N*,*N*-dimethylphenyl)-2,6-diphenyl-pyrylium perchlorate,[16] a dinuclear complex of rhodium,[17] 1-butyl-3-(4-nitro-phenylazo)-phenylthiourea[18] and UVM-7[19] were synthesised according to known procedures.

2.2 General techniques and characterisation

The XRD, TG analysis and TEM microscopy techniques were employed to characterise the materials. X-ray measurements were taken in a Bruker AXS D8 Advance diffractometer using CuKα radiation. The thermogravimetric analyses were carried out in TGA/SQTA 851e Mettler Toledo equipment, using an oxidant atmosphere (air, 80 mL min^{-1}) with a heating programme consisting in a heating ramp of 20 °C per minute from 293 K to 1273 K, and an isothermal heating step at this temperature for 15 minutes. The transmission electron microscopy (TEM) images of the particles were obtained with a Philips CM10 operating at 20 keV. The samples for TEM were prepared by spreading a drop of nanoparticles solution in decane onto standard carbon-coated copper grids (200 mesh).

2.3 Pigment preparation procedure

2.3.1 General procedure. A dye solution containing a certain amount of dye in the appropriate solvent was added to a suspension of the corresponding inorganic support and the suspension was stirred for 24 h to guarantee the maximum dye adsorption in the material. Then the solvent was removed under reduced pressure (dichloromethane or ethanol) or filtration (water) to obtain the final sensing material.

2.3.2 Pigments preparation and characterisation. *Synthesis of material 1*: dye: phenol red (10 mg, 0.0282 mmol), solvent: dichloromethane (10 mL), support: UVM-7 (500 mg). TGA: 19.3 mg dye per g solid.

Synthesis of material 2: dye: 2,6-diphenyl-4-(2-(4-*N*,*N*-dimethylaminophenyl)vinyl)-pyryliumtetrafluoroborate (10 mg, 0.0220 mmol), solvent: dichloromethane (10 mL), support: UVM-7 (500 mg). TGA: 22.8 mg dye per g solid.

Synthesis of material 3: dye: dimethyl yellow (14 mg, 0.0621 mmol), solvent: ethanol (30 mL), support: UVM-7 (686 mg). TGA: 22.1 mg dye per g solid.

Synthesis of material 4: dye: 4-(4-*N*,*N*-dimethylphenyl)-2,6-diphenylpyryliumperchlorate (17.5 mg, 0.0388 mmol), solvent: dichloromethane (10 mL), support: UVM-7 (232.5 mg). TGA: 81.1 mg dye per g solid.

Synthesis of material 5: dye: dinuclear rhodium complex (18 mg, 0.0186 mmol), solvent: dichloromethane (10 mL), support: silica gel (305.0 mg). TGA: 45.5 mg dye per g solid.

Synthesis of material 6: dye: malachite green (14 mg, 0.0384 mmol), solvent: ethanol (30 mL), support: UVM-7 (686 mg). TGA: 22.8 mg dye per g solid.

Synthesis of material 7: dye: malachite green (10 mg, 0.0274 mmol), solvent: ethanol (30 mL), support: alumina (500 mg). TGA: 20.7 mg dye per g solid.

Synthesis of material 8: dye: 1-butyl-3-(4-nitro-phenylazo)-phenylthiourea (17.5 mg, 0.0490 mmol), solvent:

dichloromethane (10 mL), support: UVM-7 (232.5 mg). TGA: 73.0 mg dye per g solid.

Synthesis of material 9: dye: carminic acid (196.96 mg, 0.4000 mmol), solvent: water (20 mL), support: UVM-7 (500 mg). TGA: 50.2 mg dye per g solid.

Synthesis of material 10: dye: *m*-cresol purple (14 mg, 0.0366 mmol), solvent: ethanol (30 mL), support: UVM-7 (686 mg). TGA: 22.6 mg dye per g solid.

Synthesis of material 11: dye: *m*-cresol purple (10 mg, 0.0260 mmol), solvent: ethanol (30 mL), support: alumina (500 mg). TGA: 20.3 mg dye per g solid.

Synthesis of material 12: dye: curcumin (17.5 mg, 0.0475 mmol), solvent: dichloromethane (10 mL), support: UVM-7 (232.5 mg). TGA: 73.3 mg dye per g solid.

Synthesis of material 13: dye: br-cresol purple (14 mg, 0.0259 mmol), solvent: ethanol (30 mL), support: UVM-7 (686 mg). TGA: 20.9 mg dye per g solid.

Synthesis of material 14: dye: br-cresol purple (10 mg, 0.0185 mmol), solvent: ethanol (30 mL), support: alumina (500 mg). TGA: 20.6 mg dye per g solid.

Synthesis of material 15: dye: phenolphthalein (14 mg, 0.0440 mmol), solvent: ethanol (30 mL), support: alumina (500 mg). TGA: 25.6 mg dye per g solid.

Synthesis of material 16: dye: litmus (50 mg, 0.2347 mmol), solvent: water (20 mL), support: UVM-7 (500 mg). TGA: 51.3 mg dye per g solid.

2.4 Preparation of chicken samples, colorimetric array preparation and storage conditions

Chicken breast fillets were acquired from a local poultry meat company (Pollos Planes S.L., Valencia, Spain). Chicken fillets (*ca.* 250 g) were packaged in boxes with MAP (30% CO_2 and 70% N_2) using a packer Smart 300 model no. 7110150 with a film of OPALEN HB 45 AF, and were kept refrigerated at 4 ± 1 °C. Thirteen dyes in different supports (a total of sixteen different sensing systems) were selected for the colorimetric sensor array, located inside the box close to the chicken samples. In addition, the colorimetric array was also packaged in the absence of chicken as a control. Studies with the chicken samples were repeated three times.

2.5 Data collection

Photographs of the trays were obtained at predetermined time intervals of 0, 3, 5, 7, 10 and 12 days post-storage. Photographs were taken by employing a light box built with polyurethane with focuses on the right and the left sides. Photographs of the different samples were always taken at the same time. The array data were collected with the Photoshop Pro 5 software by taking the RGB and Lab values from the corresponding photographs.

2.6 Statistical analysis

Principal components analysis (PCA) was carried out with the Solo 6.2 software (eigenvector Research Incorporated, WA, USA). Autoscale preprocessing and singular value decomposition (SVD), *i.e.*, an algorithm, were used to obtain a general solution to the problem of finding pseudoinverses. Partial least squares studies (PLS) were carried out with the Solo 6.2 software (eigenvector Research Incorporated, WA, USA). The SIMPLS algorithm was used for the PLS, which was developed by Sijmen de Jong.[20] This method relies on the orthogonalisation of a Krylof sequence to calculate the PLS weights. An autoscale was used as the preprocessing method; prior to building the model, cross-validation was used to evaluate the adequacy of the experimental data and to select the quantity of latent variables.

3. Results and discussion

3.1 Preparing the indicators

Chicken decay is accompanied by the production of several microbiologically induced biochemical processes which generate a wide variety of volatile compounds, including hydrogen sulfide, dimethyl disulfide, indole, lactic acid, acetic acid, other fatty acids (propionic, isobutyric, isovaleric, *n*-butyric), organic volatiles (strains or branched primary and secondary C2–C5 alcohols, C6–C8 hydrocarbons, C3–C4 ketones), diacetyl–acetoin, putrescine, cadaverine, tyramine, and other biogenic amines and ammonia.[21]

Typically, electronic noses are based on sensors limited to the weakest and least specific intermolecular interactions, primarily van der Waals and the physical adsorption interactions between the sensor and the analyte. Thus, they offer limited sensitivity for the detection of compounds at low concentrations and reduced selectivity to discriminate between compounds in natural complex matrixes. In contrast, optoelectronic noses usually focus on chemical sensors with both high sensitivity and high selectivity, and rely on the full range of intermolecular interactions (bond formation and coordination, acid–base interactions, hydrogen bonding, charge transfer and π–π molecular complexation, dipolar and multipolar interactions, *etc.*). Moreover, the possible and typical lack of reversibility associated with strong interactions is not a problem when it comes to designing low-cost disposable arrays of sensors, which are not integrated into the readout device.[12]

Inspired by previously reported optoelectronic noses and based on our own experience in designing colorimetric probes, we chose a total of 13 dyes (see Fig. 1). These include pH indicators (phenolphthalein, malachite green, *m*-cresol purple, phenol red, br-cresol purple, dimethyl yellow), Lewis acids (dinuclear rhodium complex), hydrogen bonding derivatives (1-butyl-3-(4-nitro-phenylazo)-phenylthiourea) and reactants reactive to the presence of sulfur-containing and amine functional groups (2,6-diphenyl-4-(2-(4-*N*,*N*-dimethylaminophenyl) vinyl)-pyryliumtetrafluoroborate and 4-(4-*N*,*N*-dimethylphenyl)-2,6-diphenylpyrylium perchlorate). Moreover, some natural dyes were tested (curcumin, carminic acid, litmus).

Dyes were included in a suitable support to design systems that are responsive to the volatile compounds generated during chicken spoilage. UVM-7 mesoporous silica materials were used as supports given their versatility, optical transparency in the visible range and increased dye stability. Similar dye-containing materials have been reported to be suitable supports in vapour detection.[22] UVM-7 typically has a surface of 1200 $m^2\ g^{-1}$ and is formed by ordered small (12–17 nm) mesoporous particles that generate a bimodal pore system of 3.0–3.2 nm mesopores and 20–70 nm textural pores that improve diffusion.[19] Besides, basic alumina (particle size 63–200 μm, specific surface 120 $m^2\ g^{-1}$) was

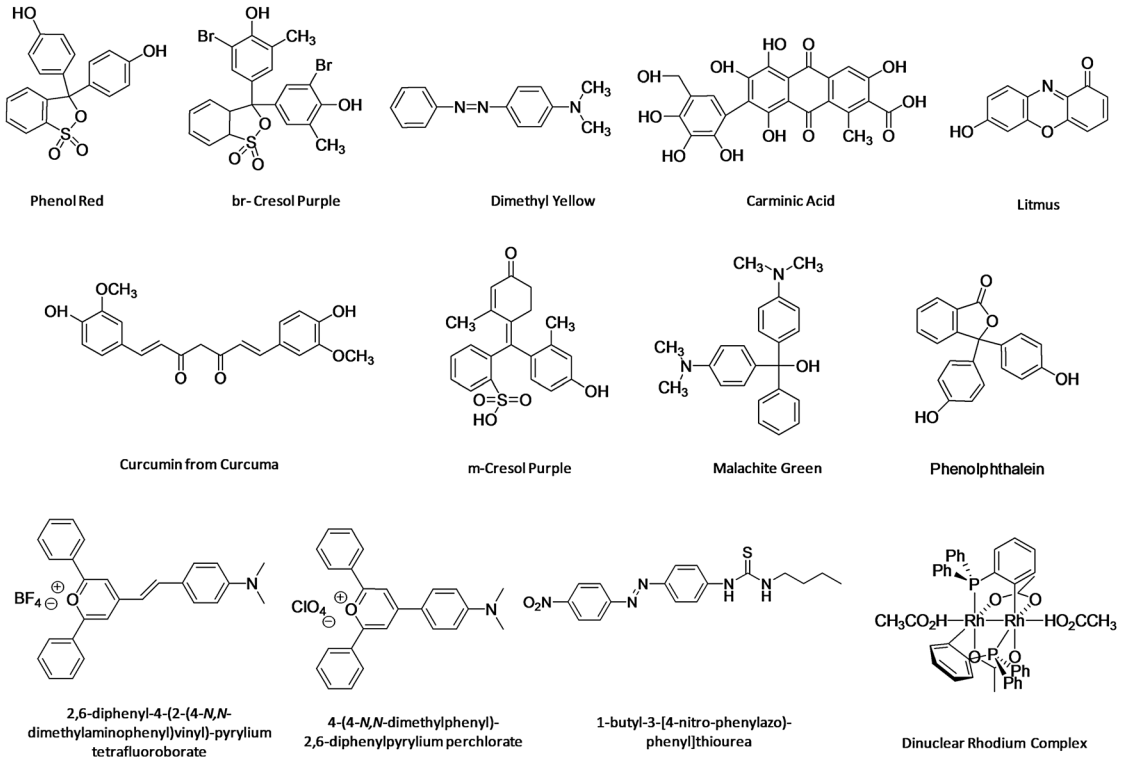

Fig. 1 Chemical structures of the dyes studied.

tested as a support for four pH indicators (phenolphthalein, *m*-cresol purple, br-cresol purple and malachite green) as an approach to improve the array response to the volatile acids generated during chicken ageing. Silica gel was also employed as a support for the dinuclear rhodium complex.

Dyes were incorporated into inorganic solids by simply stirring the corresponding dye solution (dichloromethane, ethanol or distilled water, depending on the dye) in the presence of the support for 24 h to guarantee maximum dye adsorption, followed by solvent removal. All the sensing materials were characterised by the thermogravimetric analyses (TGA). In addition, for the UVM-7-based compounds XRD and TEM characterization techniques were also used.

TGA was employed to determine the organic content. Table 1 summarises the amount of dye contained in the final supports calculated from the weight loss observed due to the combustion of the organic groups (the corresponding dye) between 200 °C and 800 °C. In general, an organic loading of between 2% and 8% was observed, corresponding to 0.1–0.2 mmol per g of solid. Similar loading values have been observed in other mesoporous materials.[23]

X-ray powder diffraction patterns of dye-loaded UVM-7 supports show the characteristic intense peak at *ca.* $2\theta = 2^\circ$ (indexed to the (100) reflection of a MCM-41-like hexagonal cell), confirming that the indicator loading process did not affect the structure of the silica matrix. In addition to this intense peak, two additional smaller peaks assigned to overlap (110) and (200) reflections of a typical hexagonal cell can be observed. The bimodal pore array of the UVM-7-based solids was clearly seen through the TEM images (see Fig. 2) in whose structure, nanometric particles joined together in micrometric conglomerates, giving rise to characteristic textural and mesoporous porosity, can be observed.

Table 1 Thermogravimetric analysis of the chromogenic sensing materials

Comp.	Dye	Support	g dye per 100 g solid	mmol dye per g solid
1	Phenol red	UVM-7	1.926	0.054
2	2,6-Diphenyl-4-(2-(4-*N*,*N*-dimethylaminophenyl)vinyl)-pyryliumtetrafluoroborate	UVM-7	2.280	0.050
3	Dimethyl yellow	UVM-7	2.206	0.098
4	4-(4-*N*,*N*-Dimethylphenyl)-2,6-diphenylpyryliumperchlorate	UVM-7	8.114	0.180
5	Dinuclear rhodium complex	Silica	4.551	0.049
6	Malachite green	UVM-7	2.278	0.062
7	Malachite green	Alumina	2.069	0.057
8	1-Butyl-3-(4-nitro-phenylazo)-phenylthiourea	UVM-7	7.304	0.205
9	Carminic acid	UVM-7	5.024	0.102
10	*m*-Cresol purple	UVM-7	2.264	0.059
11	*m*-Cresol purple	Alumina	2.032	0.053
12	Curcumin	UVM-7	7.329	0.199
13	br-Cresol purple	UVM-7	2.092	0.039
14	br-Cresol purple	Alumina	2.060	0.038
15	Phenolphthalein	Alumina	2.558	0.080
16	Litmus	UVM-7	5.128	0.241

3.2 Chromogenic array

The array was prepared by placing approximately 3 mg of each material into a ELISA microplate to obtain a 4 × 4 array (16 sensing materials). Chicken breast fillets, together with the chromogenic array, were packaged in polystyrene boxes under 30% CO_2 and 70% N_2 modified atmosphere packaging conditions (an almost maximum inhibition of aerobic floras is

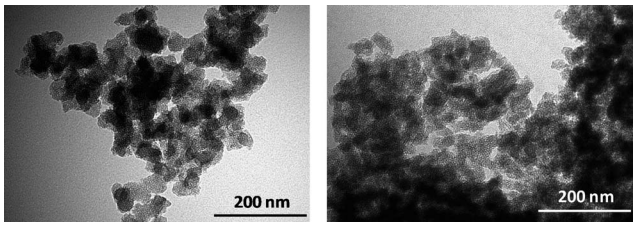

Fig. 2 TEM images of calcinated UVM-7 (left) and 3 (right).

achieved with a carbon dioxide concentration of 25%).[3] They were kept refrigerated at 4 °C throughout the experiment. Three independent samples were tested simultaneously to check the reproducibility of the dye response. The same sensing array in the absence of chicken was employed as a control, which showed minor colour variations throughout the experiment. We also observed that there was not any variation in the colour of the indicators due to changes in the temperature. A light box under controlled illumination conditions was used to obtain photographs of the array inside the trays, while the colour coordinates Lab and RGB were measured from the photographs with an image processing software (Photoshop).

Difference maps were obtained by the difference of the red, green and blue (RGB) of each compound from day n and the initial values measured on day 0. The subtraction of the two images yields a difference vector of $3N$ dimensions where N is the total number of compounds; for our 4×4 array, this difference vector was 48 dimensions (*i.e.*, 16 changes in the red, green, and blue colour values), and each dimension ranged from −255 to 255, so that an RGB value of (0,0,0) would be black, whereas values of (255,255,255) would be white. To facilitate visualisation only, the colour palette of the difference map can be enhanced by expanding the colour range from 0–100 to 0–255; any RGB change of <4 would be treated as background noise and ignored, while changes of >100 would map to 255. The difference vector is conveniently visualised in Fig. 3 as a map of the absolute values of the colour changes. For clarity purposes, the materials distribution in the array has been incorporated into the day 0 array. Day 0 shows the typical black colour corresponding to the 0,0,0 RGB coordinates. At a glance, Fig. 3 clearly shows the presence of the characteristic colour fingerprints for each day, thus confirming the possibility of using this array to monitor the chicken ageing process. We emphasise two tendencies in colour differences: the fact that almost all the dyes change colour and the enhanced colour change strength during ageing. The former indicates that all the dyes are affected by atmospheric changes during the ageing process, and they all contribute to outline the patterns. The latter, that is, more intense changes during ageing, agree with a preferential interaction of the dyes with the metabolites generated during the chicken decaying.

As noted above, the use of MAP in foods offers increased protection against perishable food due to the suppression of aerobial bacterial spoilage and, in general, to a significant reduction of the growth of other typical bacteria in chicken spoilage, such as lactic acid bacteria, enterobacteriae and yeasts. Although pseudomonas are the main species under aerobic conditions,[24] CO_2-containing atmospheres delay the development of typically aerobic spoilage-type microflora; flora is

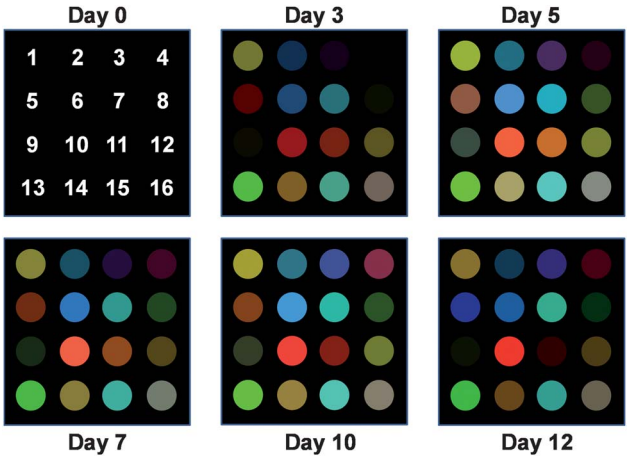

Fig. 3 Colour change profiles after exposure to the atmosphere generated by the chicken ageing process. Numbers indicate the day after packing.

replaced with CO_2-resistant organisms, such as lactic acid bacteria and related genera, but enterobacteriaceae can form a substantial portion of flora.[25] The metabolites generated during ageing depend on flora; while lactic acid bacteria produces only minor changes in flavour, pseudomonas and enterobacteriaceae produce the degradation sensation strongly associated with the generation of sulfur-containing metabolites.[26] Typically, chicken refrigerated under 30% CO_2–70% N_2 MAP conditions reaches its limit of acceptability at around days 10–12, although sensorial decaying, biogenic amines and other off-odour-generating substances are noted at around days 5–7.[25,27,28]

3.3 PCA statistical analysis

Colour differences were also analysed using PCA. This is a powerful linear unsupervised pattern recognition method. PCA is an efficient approach to diminish the dimensionality of a dataset.[29] Typically, PCA decomposes the primary data matrix by projecting the multi-dimensional dataset onto a new coordinate base formed by the orthogonal directions with data maximum variance. The eigenvectors of the data matrix are called principal components and are not intercorrelated. The principal components (PCs) are ordered so that PC1 displays the largest amount of variance, followed by the next largest, PC2, and so forth. The main feature of a PCA is the coordination of the data in the new base (scores plot) and the contribution to each component of the sensors (loads plot). Lab-based colour data were used to perform the PCA analysis. Unlike RGB, the Lab system offers a uniform non-linear colour system in which equally perceived colour differences correspond to equal distances in the Euclidean space. Thus Lab is more adequate than systems such as RGB to study colour differences on surfaces.[30] Only chroma coordinates (a and b) were employed in the statistical analysis due to the high dispersion in lightness (L) generated by the data-capturing system (photographs of the array inside the package). PC scores were then used in the discrimination analysis to assign each sample to a particular group. The original variables, in this case, were the responses of the 16 sensing materials used in the sensor array. All 32

dimensions (*i.e.*, 16 *a* coordinates and 16 *b* coordinates) would take one of the 256 possible values (from −128 to 128). The theoretical limit of discrimination would equal the number of possible patterns, *i.e.*, 256. However, since the Lab vector components extracted from the difference image of the sensor array did not cover the full range of 256, the practical limit of discrimination would be much lower, which varied with analytes.

PCA was used here as a simple method to project data to a three-dimensional plane. The mean centering pre-processing technique was applied to a dataset of 18 measurements (*i.e.*, 6 sampling days × 3 replicates) and 32 colour features. A PCA study of the full set of patterns revealed a high degree of dispersion among the independent dimensions created by the linear combinations of the *a*, *b* responses of the 16 dyes used in these arrays. The first principal component contained only 50.8% of the variance of the data. The first two components represented 67.57% of the total variance. The first five PCs explained 87.49% of the variance, whereas nine PCs were needed to account for 95% of the variance (Fig. 4). This large number of independent dimensions compared to other systems is in agreement with the wide range of chemical responsive compounds that employ several forms of intermolecular interactions between dyes and the volatile compounds generated during the chicken decay. This increasing dimensionality also helps discriminate among highly related samples (*e.g.*, different days) of the complex matrixes (meat ageing).

Although a large number of dimensions is required to explain the total variance, PCA captured 78.8% of the variance observed in the experiment in the first three PCs, which are plotted on the *x*, *y* and *z* axes, and represent the largest fraction of overall variability in the samples. Fig. 5 shows the resulting PCA for the six sampling days (three replicates) when using all the dyes (16 × 2 coordinates per dye). As observed, it was possible to discriminate among these days. When the control data were introduced into the PCA analysis, all the days were situated around day 0, which is in agreement with the systems' capacity to differentiate the control of the chicken-exposed arrays.

Furthermore, we calculated the differences in the mean scores on each day (Table 2). An exact correlation of the array colour changes with the 3D graph of the PCA graphics was not possible since a large number of indicators contributed to each PC and six PCs were needed to explain 90% of the total variance (9 for 95%). Nevertheless, some conclusions can be drawn from the statistical

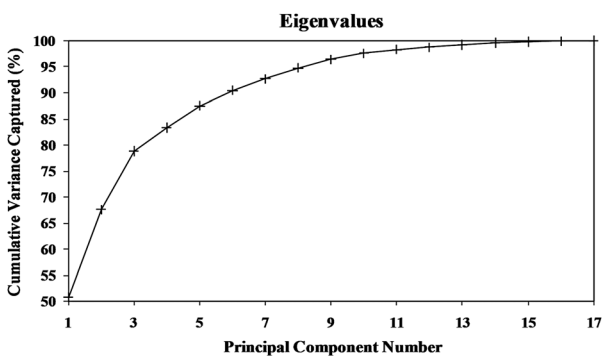

Fig. 4 The cumulative variance captured as a function of the number of principal components retained in the model.

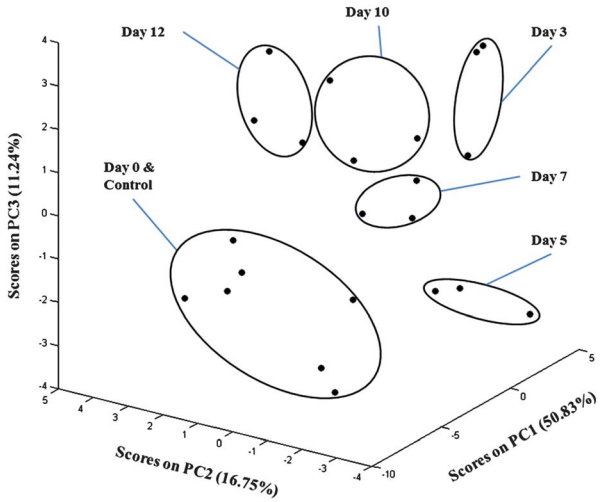

Fig. 5 The principal component analysis (PCA) score plot for the diverse chicken ageing days. Data shown for three different trials.

data. From packaging (day 0) until day 3, a strong variation was noted in PC1. This component accumulated a maximum variance, and Fig. 6 (*vide infra*) shows how this component participated mainly with pH indicators, offering less contribution from the other compounds.

Table 2 Differences of mean scores on each day by components

Days	PC1	PC2	PC3
3–0	8.826	−3.432	3.334
5–3	1.879	0.765	−5.422
7–5	−0.789	1.923	1.931
10–7	0.812	1.186	1.412
12–10	−0.590	2.405	0.135

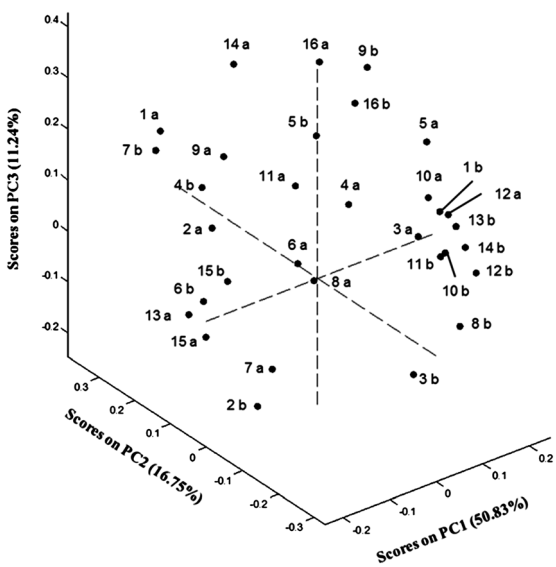

Fig. 6 Loading analysis related to sensing materials. The number indicates the material as listed in Table 1 and the letter the chroma coordinate (*a* or *b*).

The decaying process was followed mainly by PC2 and PC3, where PC3 presented stronger variations on days 3 to 5, and PC2 from days 10 to 12, with a similar displacement noted in both components from days 5 to 10. This suggests that the biochemical processes and volatile concentrations before day 5 differ from those of days 10–12, probably due to glucose consumption, to the initiation of amino acids and fats metabolisation, and to microbiological flora changes.[5,25,27,31] Once more, we must note that PC2 accumulated more variance than PC3, which is in agreement with our preferential monitoring of the spoilage process over the final days, although the array was also able to monitor intermediate decaying.

The loading analysis helped identify the probes responsible for discrimination in the current pattern file. A loading plot of the loading factors associated with the sensing materials is shown in Fig. 6. Most compounds are represented in the first three PCs. Sensing materials 6, 10, 11, 13 and 15 were mainly captured by PC1, while materials 3, 4 and 8 were captured by PC2. Sensing materials 2, 9 and 16 contributed mainly to PC3. Additionally, the other sensing systems were captured by PC1 and PC2 or PC2 and PC3, such as 1, 7 and 5, 14, respectively.

Some additional information can be obtained from each indicator's contribution to the PC. As noted above, while PC1 received the active participation of pH indicators, PC3, which offered the main changes since the beginning of the ageing process, was mainly influenced by compounds with a capacity to respond to certain metabolites (materials 2 and 5) and by supports containing natural products (compounds 9, 12 and 16). PC2 was mainly influenced by 4, 5 and 8 based on the solids-containing receptor groups that were able to interact with metabolites such as amines, carboxylic acids or other possible nucleophilic molecules originating during the chicken ageing process.

3.4 PLS statistical analysis

The PCA study has shown that the data from the optoelectronic nose clustered according to the time and helps obtain a good classification model. In this section, we were also interested in analysing whether the data taken from the optoelectronic nose could be used to predict ageing times. In order to achieve this goal, the Partial Least Square (PLS) regression technique was used. The PLS is a multivariate projection method that models the relation between an array of dependent variables (Y) and another array of independent variables (X). The principle of the technique PLS is to find the components of the matrix of input (X) that describe relevant variations in input variables as much as possible, while achieving the highest correlation with the objectives (Y) and providing the lowest weight to variations that are irrelevant or related to noise at the same time.[32]

According to cross-validated variance studies, five latent variables have been used for this study. A PLS prediction model of ageing days was created with the chroma colour coordinates obtained from the chromogenic arrays. Fig. 7 shows the PLS graph in which the measured *vs.* the predicted values of the ageing time were plotted. Hence the measured values represent the real ageing date of poultry, while the predicted values are the values calculated according to the PLS algorithm. Both the measured and predicted values were plotted together to evaluate the accuracy

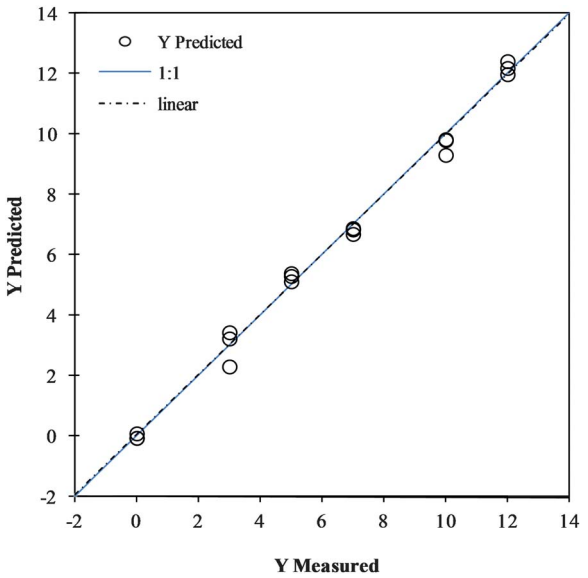

Fig. 7 The plot score of the prediction model of chicken ageing for the calibration set and linear fitting using all the sensing materials.

and precision of the created prediction models. A preliminary evaluation may be made by a visual inspection of the difference between the measured and predicted values. However, a more rigorous analysis is achieved by a linear fitting of the experimental points. Here by using a simple linear model, namely $y = p1x + p2$, a fitting line and also fitting parameters ($p1$, $p2$ and regression coefficient) were obtained. Parameters $p1$ (slope of the fitting line) and $p2$ (intercept with the y axis) represent accuracy in prediction; meanwhile, the regression coefficient can relate to the PLS model's precision. Ideally, the predicted values should lie along the diagonal line, indicating that the predicted and actual values are the same. Our PLS prediction model for ageing gave values of 0.9937, 0.0389 and 0.994 for the slope ($p1$), the intercept ($p2$) and the regression coefficient (R^2), respectively, which is in agreement with a good fit between the predicted and measured values.

Finally, although a high dimensionality system, such as the array used for an optoelectronic nose, is well suited for classifying complex systems (such as the chicken decaying process with a 2-day interval), the design of a final system that proves useful for consumers should be easy-to-use and ought to be ideally incorporated into trays. This requires a simpler approach and, for instance, a stick with only one or two dyes indicating freshness would be more appropriate. In order to achieve this goal, we selected compounds 5 and 14, and established three categories, 0–3 (fresh chicken), 5–7 (beginning of decay) and 10–12 (non-fresh chicken). As Fig. 8 depicts, a clear differentiation of colour

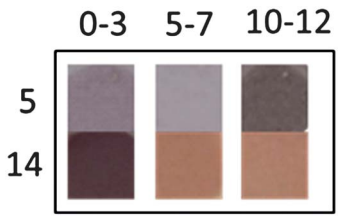

Fig. 8 The optical image of sensing materials 5 and 14 during chicken ageing.

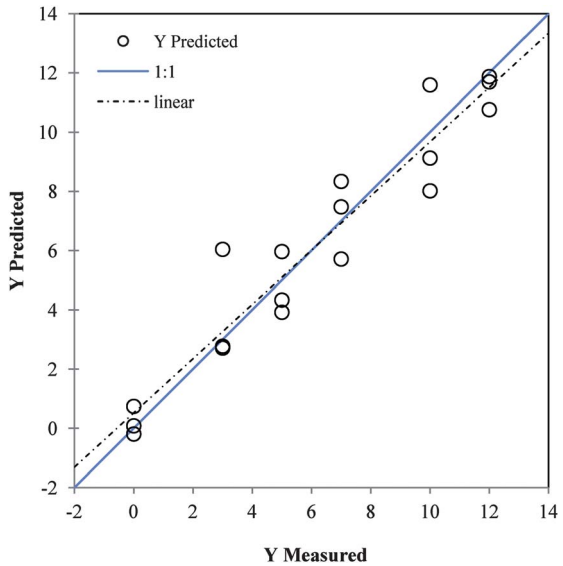

Fig. 9 The plot score of the prediction model of chicken ageing for the calibration set and linear fitting using sensing materials 5 and 14.

can be found, thus opening up the possibility of employing these or similar systems as visual probes inside chicken packages. Also a PLS ageing prediction model has been performed by only considering the sensing materials 5 and 14. Fig. 9 shows that the model decreases its accuracy and it is not able to differentiate clearly the ageing process with two-day intervals, especially in the intermediate points. By using the linear model $y = p1x + p2$, the two indicators model gave values of 0.916, 0.521 and 0.916 for the slope ($p1$), the intercept ($p2$) and the regression coefficient (R^2), respectively. These values are significantly worse in comparison with the model using 16 indicators (see Fig. 7), although it might be acceptable for some applications.

4. Conclusions

A new optoelectronic nose for monitoring chicken ageing inside MAPs has been developed. This array is based on sixteen chromogenic sensing materials developed by the incorporation of thirteen dyes into three inorganic supports with diverse acidities and topologies (UVM-7, alumina and silica gel). The selected dyes included pH indicators, Lewis acids, hydrogen-bonding derivatives and reactants reactive to the presence of sulphur- and amine-containing derivatives, which confirm an effective set of materials for monitoring decaying processes in chicken. The array is able to differentiate samples with a 2-day difference in the storage time, which offers a characteristic colorimetric fingerprint. The PCA statistical analysis of the results confirmed the system's ability to classify samples according to chicken freshness and to obtain a visual samples clustering in a 3D diagram without errors or misclassifications. PC2 and PC3 were influenced by the chicken-induced changes in the atmosphere. Colour differences were also employed to create a PLS model, which shows a high quality fit between the predicted and observed values, as well as a regression coefficient (R^2) of 0.994. A shortened version of the array based on two sensing materials was used for a "naked eye" simplified classification. The results suggest the feasibility of this system to develop optoelectronic noses that monitor food freshness.

Acknowledgements

The financial support from the Spanish Government (projects CIT-060000-2008-14 and MAT2009-14564-C04-01), the Generalitat Valenciana (Valencian Regional Government; project PROMETEO/2009/016) and the UPV (PAID-06-010-2414) is gratefully acknowledged. Y.S. also thanks the Spanish Ministry of Science for a PhD fellowship.

Notes and references

1 *Livestock and Poultry: World Markets and Trade*, United States department of agriculture. Foreign agricultural service, April 2011.
2 D. M. Anang, G. Rusul, F. H. Ling and R. Baht, *Int. J. Food Microbiol.*, 2010, **144**, 152; A. Hinton and K. D. Ingram, *J. Food Prot.*, 2005, **68**, 1462.
3 L. E. Jeremiah, *Food Res. Int.*, 2001, **34**, 749.
4 L. R. Freeman, G. J. Silverman, P. Angelini, C. Merrit and W. B. Esselen, *Appl. Environ. Microbiol.*, 1976, 222.
5 D. I. Ellis and R. Goodacre, *Trends Food Sci. Technol.*, 2001, **12**, 414; G. Vinci and M. L. Antonelli, *Food Control*, 2002, **13**, 519; T. M. Lovestead and T. J. Bruno, *Food Chem.*, 2010, **121**, 1274.
6 G. M. Bota and P. B. Harrington, *Talanta*, 2006, **68**, 629; R. Grau, A. J. Sanchez, J. Giron, E. Iborra, A. Fuentes and J. M. Barat, *Food Res. Int.*, 2011, **44**, 331; A. Sahar, T. Boubellouta and E. Dufour, *Food Res. Int.*, 2011, **44**, 471; M. Lin, M. Al-Holy, M. Mousavi-Hesary, H. Al-Qadiri, A. G. Cavinato and B. A. Rasco, *Lett. Appl. Microbiol.*, 2004, **39**, 148.
7 F. Li, L. Zhou, J. Zhang, X. Sun, W. Niu, Y. Zhang, Q. Song, Z. Li and C. Wan, CN101806741-A, Univ Jiangnan.
8 R. Martínez-Máñez and F. Sancenón, *Chem. Rev.*, 2003, **103**, 4419; V. Amendola, L. Fabbrizzi and L. Mosca, *Chem. Soc. Rev.*, 2010, **39**, 3889; D. T. Quang and J. S. Kim, *Chem. Rev.*, 2010, **110**, 6280; V. Amendola, M. Bonnizoni, D. Esteban-Gomez, L. Fabbrizzi, M. Licchelli, F. Sancenón and A. Taglietti, *Coord. Chem. Rev.*, 2006, **250**, 1451; X. Chen, Y. Zhou, X. Peng and J. Yoon, *Chem. Soc. Rev.*, 2010, **39**, 2120; G. J. Mohr, *Anal. Bioanal. Chem.*, 2006, **386**, 1201.
9 J. P. Kerry, M. N. O'Grady and S. A. Hogan, *Meat Sci.*, 2006, **74**, 113.
10 S. A. Piletsky, S. P. J. Higson and F. Davis, WO2006024848–A1, Univ Cranfield.
11 N. A. Rakow and K. S. Suslick, *Nature*, 2000, **406**, 710; S. H. Lim, J. W. Kemling, L. Feng and K. S. Suslick, *Analyst*, 2009, **134**, 2453; M. A. Palacios, R. Nishiyabu, M. Marquez and P. Azenbacher, *J. Am. Chem. Soc.*, 2007, **129**, 7538; Y. Wu, N. Na, S. Zhang, X. Wang, D. Liu and X. Zhang, *Anal. Chem.*, 2009, **81**, 961.
12 M. C. Janzen, J. B. Ponder, D. P. Bailey, C. K. Ingison and K. S. Suslick, *Anal. Chem.*, 2006, **78**, 3591.
13 B. A. Suslick, L. Feng and K. S. Suslick, *Anal. Chem.*, 2010, **82**, 2067; X. Huang, J. Xin and J. Zhao, *J. Food Eng.*, 2011, **105**, 632; P. Anzenbacher, P. Lubal, N. A. Palacios and M. E. Kozelkova, *Chem. Soc. Rev.*, 2010, **39**, 3954.
14 J. V. Ros-Lis, B. García, D. Jiménez, R. Martínez-Máñez, F. Sancenón, J. Soto, F. Gonzalvo and M. C. Valldecabres, *J. Am. Chem. Soc.*, 2004, **126**, 4064; J. V. Ros-Lis, R. Martínez-Máñez, K. Rurack, F. Sancenón, J. Soto and M. Spieles, *Inorg. Chem.*, 2004, **43**, 5183; J. V. Ros-Lis, M. D. Marcos, R. Martínez-Máñez, K. Rurack and J. Soto, *Angew. Chem., Int. Ed.*, 2005, **44**, 4405; J. V. Ros-Lis, R. Martínez-Máñez and J. Soto, *Org. Lett.*, 2005, **7**, 2337; E. Climent, M. D. Marcos, R. Martínez-Máñez, F. Sancenón, J. Soto, K. Rurack and P. Amorós, *Angew. Chem., Int. Ed.*, 2009, **48**, 8519; T. Abalos, D. Jiménez, R. Martínez-Máñez, J. V. Ros-Lis, S. Royo, F. Sancenón, J. Soto, A. M. Costero, S. Gil and M. Parra, *Tetrahedron Lett.*, 2009, **50**, 3885; E. Climent, C. Giménez, M. D. Marcos, R. Martínez-Máñez, F. Sancenón and J. Soto, *Chem. Commun.*, 2011, **47**, 6873; S. Royo, A. M. Costero, M. Parra, S. Gil, R. Martínez-Máñez and F. Sancenón, *Chem.–Eur. J.*, 2011, **17**, 6931.

15 B. García-Acosta, M. Comes, J. L. Bricks, M. A. Kudinova, V. V. Kurdyukov, A. I. Tolmachev, A. B. Descalzo, M. D. Marcos, R. Martínez-Máñez, A. Moreno, F. Sancenón, J. Soto, L. A. Villaescusa, K. Rurack, J. M. Barat, I. Escriche and P. Amorós, *Chem. Commun.*, 2006, 2239.
16 F. Sancenón, A. B. Descalzo, R. Martínez-Máñez, M. A. Miranda and J. Soto, *Angew. Chem., Int. Ed.*, 2001, **40**, 2640.
17 J. Esteban, J. V. Ros-Lis, R. Martínez-Máñez, M. D. Marcos, M. Moragues, J. Soto and F. Sancenón, *Angew. Chem., Int. Ed.*, 2010, **49**, 4934; M. E. Moragues, J. Esteban, J. V. Ros-Lis, R. Martínez-Máñez, M. D. Marcos, M. Martínez, J. Soto and F. Sancenón, *J. Am. Chem. Soc.*, 2011, **133**, 15762.
18 J. V. Ros-Lis, R. Martínez-Máñez, F. Sancenón, J. Soto, K. Rurack and H. Weißhoff, *Eur. J. Org. Chem.*, 2007, 2449.
19 J. El Haskouri, D. Ortiz de Zárate, C. Guillem, J. Latorre, M. Caldés, A. Beltrán, D. Beltrán, A. B. Descalzo, G. Rodríguez-López, R. Martínez-Máñez, M. D. Marcos and P. Amorós, *Chem. Commun.*, 2002, 330.
20 S. de Jong, *Chemom. Intell. Lab. Syst.*, 1993, **18**, 251.
21 M. Smolander, E. Hurme, K. Latva-Kala, T. Luoma, H.-L. Alakomi and R. Ahvenainen, *Innovative Food Sci. Emerging Technol.*, 2002, 279; R. H. Dainty, *Int. J. Food Microbiol.*, 1996, **33**, 19; G. D. García de Fernando, G. J. E. Nychas, M. W. Peck and J. A. Ordóñez, *Int. J. Food Microbiol.*, 1995, **28**, 221.
22 A. B. Descalzo, M. D. Marcos, C. Monte, R. Martínez-Máñez and K. Rurack, *J. Mater. Chem.*, 2007, **17**, 4716.
23 A. B. Descalzo, K. Rurack, H. Weisshoff, R. Martínez-Máñez, M. D. Marcos, P. Amorós, K. Hoffmann and J. Soto, *J. Am. Chem. Soc.*, 2005, **127**, 184; M. Comes, E. Aznar, M. Moragues, M. D. Marcos, R. Martínez-Máñez, F. Sancenón, J. Soto, L. A. Villaescusa, L. Gil and P. Amorós, *Chem.–Eur. J.*, 2009, **15**, 9024.
24 G.-J. E. Nuchas and C. C. Tassou, *J. Sci. Food Agric.*, 1997, **74**, 199.
25 S. M. Jiménez, M. S. Salsi, M. C. Tiburzi, R. C. Rafaghelli, M. A. Tessi and V. R. Coutaz, *J. Appl. Microbiol.*, 1997, **83**, 613.
26 G. D. García de Fernando, G. J. E. Nychas, M. W. Peck and J. A. Ordóñez, *Int. J. Food Microbiol.*, 1995, **28**, 221.
27 C. C. Balamatsia, A. Patsias, M. G. Kontominas and I. N. Savvaidis, *Food Chem.*, 2007, **104**, 1622; C. C. Balamatsia, E. K. Paleologos, M. G. Kontominas and I. N. Savvaidis, *Antonie van Leeuwenhoek*, 2006, **89**, 9.
28 M. Smolander, E. Hurme, K. Latva-Kala, T. Luoma, H.-L. Alakomi and R. Ahvenainen, *Innovative Food Sci. Emerging Technol.*, 2002, **3**, 279.
29 H. Martens and M. Martens, *Multivariate Analysis of Quality. An Introduction*, John Wiley & Sons, Inc., 2001.
30 E. J. Gilabert, *Medida del color*, Universidad Politécnica de Valencia, 2007.
31 R. H. Dainty, *Int. J. Food Microbiol.*, 1996, **33**, 19.
32 L. A. Berruela, R. M. Alonso-Salcesm and K. Héberguer, *J. Chromatogr., A*, 2007, **1158**, 196.